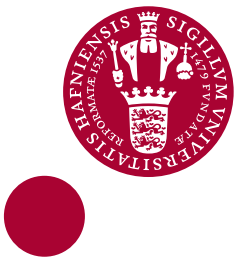

Tumor-Associated Macrophages Derived from Circulating Inflammatory Monocytes Degrade Collagen through Cellular Uptake

Madsen, Daniel Hargbøl; Jürgensen, Henrik Jessen; Siersbæk, Majken Storm; Kuczek, Dorota Ewa; Grey Cloud, Loretta; Liu, Shihui; Behrendt, Niels; Grøntved, Lars; Weigert, Roberto; Bugge, Thomas Henrik

Published in:
Cell Reports

DOI:
10.1016/j.celrep.2017.12.011

Publication date:
2017

Document version
Publisher's PDF, also known as Version of record

Report

Cell Reports

Tumor-Associated Macrophages Derived from Circulating Inflammatory Monocytes Degrade Collagen through Cellular Uptake

Graphical Abstract

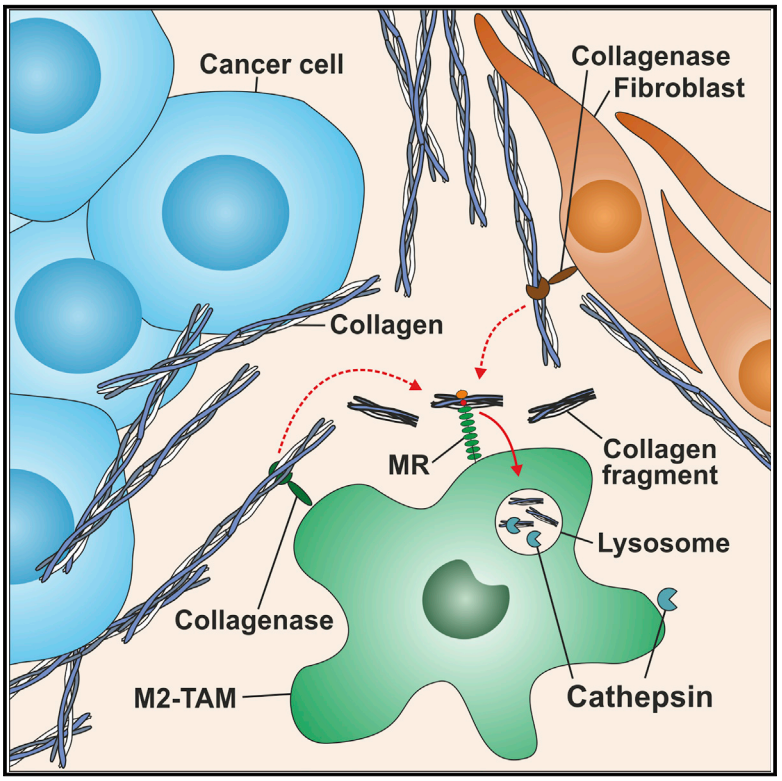

Highlights

- CCR2+ monocyte-derived tumor-associated macrophages degrade collagen in tumors
- Collagen-degrading macrophages display a matrix catabolic transcriptomic signature
- Tumor-mediated collagen degradation entails cellular uptake and lysosomal routing
- The mannose receptor mediates cellular collagen uptake by matrix-degrading cells

Authors

Daniel Hargbøl Madsen, Henrik Jessen Jürgensen, Majken Storm Siersbæk, ..., Lars Grøntved, Roberto Weigert, Thomas Henrik Bugge

Correspondence

daniel.hargboel.madsen@regionh.dk (D.H.M.), thomas.bugge@nih.gov (T.H.B.)

In Brief

Madsen et al. identify a population of tumor-associated macrophages with a distinct matrix catabolic signature as key effectors of collagen turnover during invasive tumor growth. These matrix-degrading macrophages are largely derived from CCR2+ monocytes reprogrammed by the tumor microenvironment and degrade collagen through mannose receptor-dependent cellular uptake.

Data and Software Availability

GSE107053

Madsen et al., 2017, Cell Reports *21*, 3662–3671
December 26, 2017
https://doi.org/10.1016/j.celrep.2017.12.011

CellPress

OPEN ACCESS
CellPress

Cell Reports
Report

Tumor-Associated Macrophages Derived from Circulating Inflammatory Monocytes Degrade Collagen through Cellular Uptake

Daniel Hargbøl Madsen,[1,3,4,5,*] Henrik Jessen Jürgensen,[1,5] Majken Storm Siersbæk,[6] Dorota Ewa Kuczek,[3] Loretta Grey Cloud,[1] Shihui Liu,[1] Niels Behrendt,[5] Lars Grøntved,[6] Roberto Weigert,[2,7] and Thomas Henrik Bugge[1,8,*]

[1]Proteases and Tissue Remodeling Section
[2]Intracellular Membrane Trafficking Unit
Oral and Pharyngeal Cancer Branch, National Institute of Dental and Craniofacial Research, National Institutes of Health, Bethesda, MD 20892, USA
[3]Center for Cancer Immune Therapy, Department of Haematology
[4]Department of Oncology
Copenhagen University Hospital, 2730 Herlev, Denmark
[5]The Finsen Laboratory, Rigshospitalet/Biotech Research and Innovation Centre (BRIC), University of Copenhagen, 2200 Copenhagen, Denmark
[6]Department of Biochemistry and Molecular Biology, University of Southern Denmark, 5230 Odense, Denmark
[7]Laboratory of Cellular and Molecular Biology, CCR, National Cancer Research Bethesda, MD 20892, USA
[8]Lead Contact
*Correspondence: daniel.hargboel.madsen@regionh.dk (D.H.M.), thomas.bugge@nih.gov (T.H.B.)
https://doi.org/10.1016/j.celrep.2017.12.011

SUMMARY

Physiologic turnover of interstitial collagen is mediated by a sequential pathway in which collagen is fragmented by pericellular collagenases, endocytosed by collagen receptors, and routed to lysosomes for degradation by cathepsins. Here, we use intravital microscopy to investigate if malignant tumors, which are characterized by high rates of extracellular matrix turnover, utilize a similar collagen degradation pathway. Tumors of epithelial, mesenchymal, or neural crest origin all display vigorous endocytic collagen degradation. The cells engaged in this process are identified as tumor-associated macrophage (TAM)-like cells that degrade collagen in a mannose receptor-dependent manner. Accordingly, mannose-receptor-deficient mice display increased intratumoral collagen. Whole-transcriptome profiling uncovers a distinct extracellular matrix-catabolic signature of these collagen-degrading TAMs. Lineage-ablation studies reveal that collagen-degrading TAMs originate from circulating CCR2+ monocytes. This study identifies a function of TAMs in altering the tumor microenvironment through endocytic collagen turnover and establishes macrophages as centrally engaged in tumor-associated collagen degradation.

INTRODUCTION

Invasive tumor growth causes loss of tissue architecture and organ failure (Danø et al., 1985; Liotta et al., 1983; Sloane and Honn, 1984). It involves extensive degradation of interstitial collagen, which is the most abundant extracellular matrix (ECM) component. ECM degradation allows for physical expansion and facilitates tumor growth by growth factor release from the ECM (Hynes, 2009). ECM degradation is often accompanied by deposition of a tumor-supporting ECM with altered stiffness, composition, and organization (Kaukonen et al., 2016; Lu et al., 2012; Naba et al., 2014; Schedin and Keely, 2011). Interstitial collagen is a dense network of collagen fibers stabilized by multiple inter- and intramolecular crosslinks (Linsenmayer, 1991; Ricard-Blum and Ville, 1989), forming a supramolecular structure refractory to all but a handful of proteolytic enzymes of the matrix metalloproteinase (MMP) family. These collagenases cleave collagen at a single site (Aimes and Quigley, 1995; Birkedal-Hansen, 1987; Freije et al., 1994; Hasty et al., 1987; Hotary et al., 2000, 2006; Knäuper et al., 1996; Netzel-Arnett et al., 2002; Stricklin et al., 1977) to release large collagen fragments that are internalized through the engagement of endocytic receptors of the mannose receptor (MR) family and collagen-binding β1 integrins. The internalized collagen fragments are routed to lysosomes and degraded by lysosomal cathepsins (Engelholm et al., 2003; Everts et al., 1985; Everts and Beertsen, 1992; Kjøller et al., 2004; Lee et al., 1996, 2006; Madsen et al., 2007, 2011, 2012, 2013; Martinez-Pomares et al., 2006).

Tumor-associated macrophages (TAMs) are the most abundant leukocytes in tumor stroma. TAMs derive from tissue-resident macrophages or from recruited inflammatory monocytes conditioned by the tumor microenvironment (Franklin et al., 2014; Lahmar et al., 2016; Noy and Pollard, 2014), and the density of TAMs correlates with prognosis (Biswas et al., 2013; Zhang et al., 2012).

We recently established an imaging assay that enables the visualization of cellular collagen degradation *in situ* (Madsen et al., 2013). Here, we used this assay to study endocytic turnover of interstitial collagen in the tumor microenvironment of

syngrafted and genetically induced mouse cancers. Irrespective of tumor type, endocytic interstitial collagen turnover was vigorous and mediated by cells phenotypically resembling TAMs. The cells expressed high levels of M2 markers and depended on the MR for endocytic collagen degradation. Transcriptomic profiling of fluorescence-activated cell sorting (FACS)-isolated collagen-endocytosing TAMs revealed a distinct ECM-catabolic signature, characterized by high expression of ECM-degrading enzymes and low expression of ECM proteins. Collagen-endocytosing TAMs mostly were derived from CCR2+ inflammatory monocytes recruited to the tumor microenvironment. The study establishes TAMs as mediators of tumor-associated endocytic collagen degradation.

RESULTS

Endocytic Pathway for Collagen Turnover Is Highly Active in Solid Tumors

Acid-extracted fluorescence-labeled rat-tail collagen fibrils spontaneously form collagen fiber networks when placed in connective tissue. The fate of this collagen can be followed by two-photon or confocal microscopy (Madsen et al., 2013). We injected fluorescent collagen and dextran, a lysosomal marker, into subcutaneous Lewis lung carcinoma (LLC) growing in syngeneic mice and, separately, into adjacent dermis. The mice carried a *Col1a1*-GFP transgene allowing for identification of cancer-associated and dermal fibroblasts. Multiple cells endocytosing collagen were seen in the tumors 24 hr after collagen injection, showing that the endocytic collagen degradation pathway is operative within the tumor microenvironment (Figure 1A). These collagen-endocytosing cells also endocytosed large amounts of dextran and were not fibroblasts, as determined by their lack of GFP expression (Figure 1A).

Serial z stack analysis showed that collagen-endocytosing cells were far more abundant in tumor tissue than in adjacent dermis (Figures 1A and 1B, quantified in Figure 1C). This is consistent with the high rate of collagen turnover in neoplastic tissue, as compared to normal tissue (Jones and De Clerck, 1982; Lu et al., 2012). High-level collagen- and dextran-endocytosing cells were also abundant in syngeneic B16BL6 melanoma of neural crest origin (Figure S1A) and T241 fibrosarcoma of mesenchymal origin (Figure S1B), as well as in MMTV-PymT transgene-induced mammary adenocarcinomas (Figure S1C). In all tumors, collagen-endocytosing cells had identical morphology and were not tumor-associated fibroblasts, as shown by the lack of GFP expression (Figures 1A and S1A–S1C). Taken together, this shows that the endocytic collagen degradation pathway is highly active in solid tumors, regardless of tumor cell origin, and that it is executed by a tumor microenvironment-abundant population of cells different from tumor-associated fibroblasts.

Macrophages Mediate Endocytic Collagen Degradation in Tumors

To identify cells mediating endocytic collagen degradation, we made LLC cells stably expressing dTomato fluorescent protein, and formed tumors in syngeneic *Col1a1*-GFP mice, to simultaneously visualize tumor cells and tumor-associated fibroblasts. Surprisingly, when tumors were imaged 24 hr after collagen injection, high-level collagen endocytosing cells were neither tumor cells nor tumor-associated fibroblasts (Figure 1D). An absence of collagen endocytosis by tumor cells and by tumor-associated fibroblasts was also observed when the experiment was performed using dTomato-expressing T241 fibrosarcoma cells (Figure 1E). Aligned with this, collagen-endocytosing cells expressed the macrophage marker CD11b and the M2-macrophage marker, MR, as shown by *in situ* immunostaining of LLC tumors (Figures 1F and 1G), indicating that collagen-endocytosing cells are TAMs.

To extend these findings, we analyzed single-cell suspensions from subcutaneous LLC injected with fluorescent collagen and dextran by flow cytometry (Figures 1H–1K). Consistent with the *in situ* immunostaining, most collagen- and dextran-internalizing cells expressed the pan-macrophage marker F4/80. Interestingly, these cells also frequently expressed the dendritic cell markers CD11c and MHCII, which were infrequently expressed on collagen- and dextran non-endocytosing cells (Figure 1K). This resemblance of TAMs to dendritic cells is aligned with recent findings (Lohela et al., 2014).

Collagen-Endocytosing Cells Are M2-like TAMs with a Distinct Matrix Catabolic Signature

We further characterized cells mediating endocytic collagen degradation in tumors using markers of macrophage polarization. For this, we generated subcutaneous LLC, injected fluorescent collagen, prepared single-cell suspensions 24 hr later, and isolated CD45+ and CD11b+ cells endocytosing high levels of collagen and dextran by FACS (Figure 2A). For comparison, we FACS-isolated CD45+ and CD11b+ cells not endocytosing dextran and collagen (Figure 2B). qPCR analysis of collagen- and dextran-endocytosing cells showed high expression of the M2-macrophage markers, *Mrc1* (encoding MR), *Retnla* (encoding Fizz1), and *Arg1* (encoding arginase) and, correspondingly, a low expression of the M1-macrophage marker *Nos2* (encoding iNOS) (Figure 2C).

TAMs may contribute to both ECM turnover and the construction of a tumor-specific ECM by secreting ECM components (Afik et al., 2016). To further define collagen-endocytosing TAMs, we generated subcutaneous LLC using dTomato fluorescent protein-expressing LLC cells in *Col1a1*-GFP mice, followed by injection of fluorescent collagen to enable the FACS isolation of cancer cells, tumor-associated fibroblasts, and collagen-endocytosing TAMs (Figures 2D and 2E). Each of these cell populations, as well as tumor cell suspensions prior to FACS-isolation, was then profiled by RNA sequencing (RNA-seq). The full dataset is in Table S1. Principal component analysis showed clear separation of the three cell types, with the total tumor sample placed closest to the LLC cells (Figure 2F). RNA-seq data confirmed the expression of M2-macrophage markers identified by imaging, flow cytometry, and qRT-PCR and also verified that the sorted dTomato- and GFP-expressing cells were indeed cancer cells and fibroblasts, respectively (Figure S2).

Interestingly, collagen-endocytosing TAMs differed from TAMs described by Afik et al. by low expression of collagen genes, including fibril-forming collagens, basement membrane

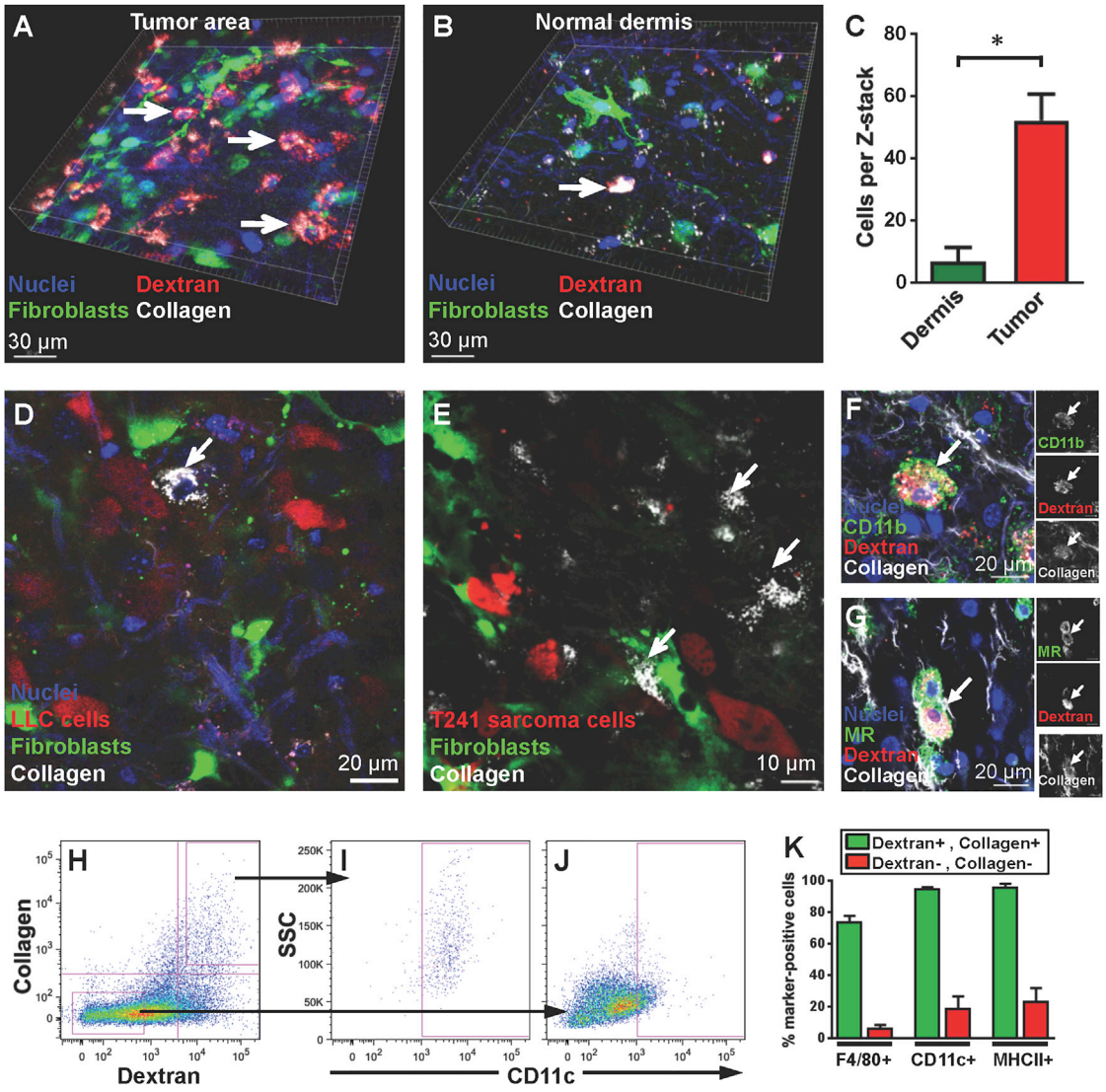

Figure 1. Tumors Are Infiltrated by High-Level Collagen-Endocytosing M2-Polarized Macrophages

(A and B) Projections of subcutaneous LLC (A) or adjacent dermal tissue (B) 24 hr after injection of fluorescent collagen and dextran into *Col1a1*-GFP reporter mice expressing GFP in fibroblasts.

(C) Quantification of high-level collagen-endocytosing cells in tumor (red bar, examples in A) or in adjacent dermis (green bar, example in B). n = 3 mice (three z stacks per mouse). Error bars, SD. *p < 0.01.

(D and E) Tumor tissue 24 hr after injection of fluorescent collagen into dTomato-expressing LLC (D) and dTomato-expressing T241 fibrosarcoma (E). Examples of high-level collagen endocytosing cells are indicated with arrows in (A), (B), (D), and (E).

(F and G) LLC *in situ* stained for CD11b (F) or MR (G) 24 hr after collagen and dextran injection. Arrows show high-level collagen-endocytosing cells positive for CD11b (F) or MR (G).

(H–K) Flow cytometry analysis of single-cell suspensions of an LLC tumor for CD11c expression by collagen- and dextran-endocytosing cells (I) or collagen- and dextran-non-endocytosing cells (J). (K) Percentages of dextran- and collagen-endocytosing cells (green bars) or dextran- and collagen-non-endocytosing cells (red bars) from tumor single-cell suspensions positive for the indicated surface markers based on flow cytometry analysis exemplified in (H)–(J). n = 4 mice. Error bars, SD.

collagens, and fibril-associated collagens with interrupted triple helices, proteoglycans, and other ECM glycoproteins, which were expressed at much higher levels in tumor-associated fibroblasts (Figure 2G). Collagen-endocytosing TAMs expressed high levels of cathepsins, which is consistent with high lysosomal degradation capacity (Figure 2H). Collagen-endocytosing TAMs also expressed the highest levels of the genes encoding the collagenases MMP-8, and MMP-13, as well as high levels of the genes encoding the gelatinase MMP-9 and the elastase MMP-12. Genes encoding MMP-3 and the collagenases MMP-2 and MMP-14 were expressed at higher levels in tumor-associated fibroblasts (Figure 2H). Finally, genes encoding fibrinolytic proteins were mostly expressed by either tumor-associated fibroblasts or the collagen-endocytosing TAMs (Figure 2H).

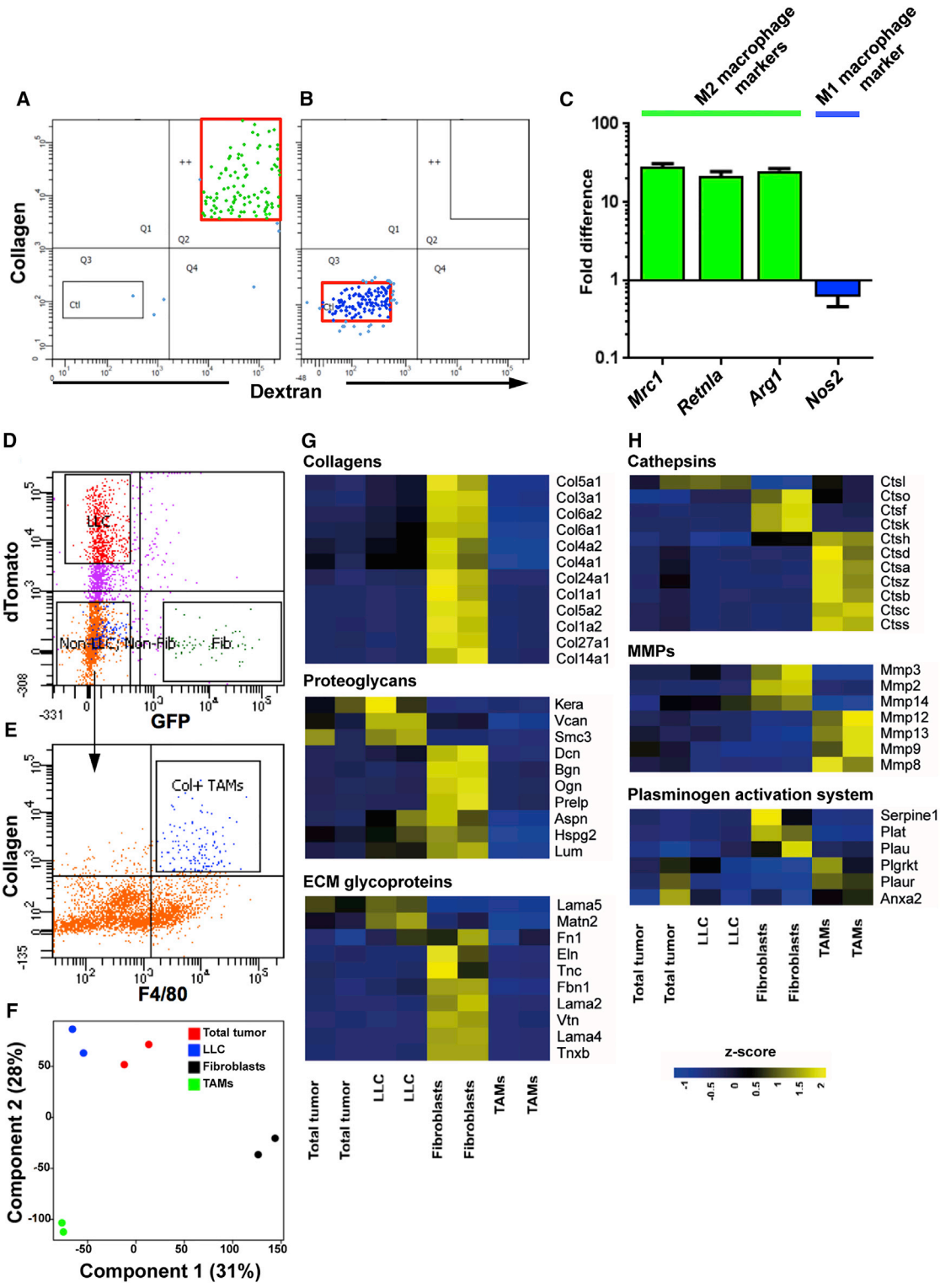

Figure 2. A Distinct ECM-Catabolic Transcriptomic Signature of Collagen-Endocytosing TAMs

(A and B) Post-sorting flow cytometry analysis of single-cell suspensions of LLC FACS sorted into CD45+;CD11b+ cells endocytosing dextran and collagen (A) or not endocytosing dextran and collagen (B).

(C) qRT-PCR analysis for M2-polarization markers (green bars) and an M1-polarization marker (blue bar). Data were generated by normalizing the expression level of dextran- and collagen-endocytosing CD45+;CD11b+ cells to dextran- and collagen-non-endocytosing CD45+;CD11b+ cells. n = 3. Error bars, SD.

(legend continued on next page)

Collagen-Endocytosing TAMs Originate from CCR2+ Monocytes

To determine the origin of collagen-degrading cells in tumors, we used a mouse strain that expresses the human diphtheria toxin (DT) receptor under control of the *Ccr2* promoter (*CCR2-depleter*$^{+/0}$ mice). This strain was crossed to *Ccr2*$^{+/RFP}$ mice, which carry a RFP reporter gene inserted into the endogenous *Ccr2* gene, to generate *Ccr2*$^{+/RFP}$;*CCR2-depleter*$^{+/0}$ bi-transgenic mice and *Ccr2*$^{+/RFP}$ littermates. This allowed for selective depletion of CCR2+ cells from tumors by the administration of DT and a simultaneous monitoring of depletion efficacy using flow cytometry. Accordingly, these mice were inoculated with LLC and treated with DT. Flow cytometry analysis of single-cell suspensions of tumors showed that CCR2+ cells constituted 21% of all cells in the tumors of DT-treated *Ccr2*$^{+/RFP}$ mice (Figure 3A), and that DT-treatment of *Ccr2*$^{+/RFP}$;*CCR2-depleter*$^{+/0}$ littermates resulted in near complete ablation of CCR2+ cells (Figure 3B). Analysis of single-cell suspensions from collagen-injected LLC tumors growing in DT-treated *Ccr2*$^{+/RFP}$ mice also revealed that about half of the collagen-endocytosing cells in tumors were CCR2+ and about half were CCR2- (Figure 3C). As expected, the CCR2+ collagen-endocytosing cells were essentially absent in DT-treated *Ccr2*$^{+/RFP}$;*CCR2-depleter*$^{+/0}$ bi-transgenic mice (Figure 3D). Interestingly, CCR2− collagen-endocytosing cells were also highly reduced after the CCR2 expression-dependent depletion (compare Figures 3C and 3D, quantified in Figure 3E), suggesting that most collagen-endocytosing CCR2− cells in tumors are derived from CCR2+ tumor-recruited monocytes.

MR Mediates Endocytic Collagen Degradation by TAMs

In situ immunostaining (Figure 1G) and transcriptomic profiling of collagen-endocytosing cells (Figure 2C) revealed a high expression of MR, a key collagen endocytosis receptor (Madsen et al., 2013; Martinez-Pomares et al., 2006). To determine the role of MR in endocytic collagen degradation in tumors, we established subcutaneous LLC in syngeneic wild-type (*Mrc1*$^{+/+}$) mice and MR-deficient (*Mrc1*$^{-/-}$) littermates, and injected fluorescent collagen into the tumors. Analysis of tumors growing in *Mrc1*$^{+/+}$ mice showed numerous cells endocytosing collagen when analyzed 24 hr later (Figure 4A). In contrast, we found very few collagen-endocytosing cells in tumors growing in *Mrc1*$^{-/-}$ littermates (Figure 4B). To further analyze the role of MR in tumor-associated collagen degradation, we affinity purified CD45+ cells from collagen-injected LLC growing in *Mrc1*$^{+/+}$ and *Mrc1*$^{-/-}$ mice and analyzed the macrophage populations by flow cytometry (Figures 4C and 4D). Consistent with the image analysis, the fraction of CD45+, CD11b+, and F4/80+ cells endocytosing high levels of collagen was dramatically reduced by loss of MR (Figure 4E). In further support of a pivotal role of MR in endocytic collagen turnover, when CD45+,CD11b+ cells from LLC were sorted into MR+ and MR− cells and cultured with fluorescently labeled collagen, MR+ cells endocytosed 11-fold more collagen than MR− cells (Figures 4F and 4G). Next, we followed the growth of subcutaneous LLC in MR-deficient mice and wild-type littermates. The tumors grew slightly slower in MR-deficient mice (Figure 4H), although the difference did not reach statistical significance. When analyzing the collagen content of the tumors, we observed a striking 2.7-fold increase in collagen in tumors of MR-deficient mice (Figures 4I and 4J).

DISCUSSION

Tumors are rapidly expanding pseudo-organs that efficiently dissolve existing ECM structures. Accordingly, we found that the endocytic pathway for interstitial collagen degradation is highly active in tumors of multiple different origins, and in all tumors, was executed by cells with characteristics of TAMs. These collagen-degrading TAMs largely originated from circulating CCR2+ monocytes recruited to the tumor microenvironment, and MR was identified as the principal collagen endocytosis receptor on these cells.

TAMs are central orchestrators of a diverse array of processes critical to tumor initiation, propagation, and dissemination. These include suppression of anti-tumor cytotoxic T cells, promotion of tumor cell growth, motility, invasion, intravasation, angiogenesis, and ECM deposition (Afik et al., 2016; Gocheva et al., 2010; Hughes et al., 2015; Lahmar et al., 2016; Lewis et al., 2016; Noy and Pollard, 2014; De Palma et al., 2005). Many of these functions are ascribed to the M2-polarization of TAMs, and therapeutic approaches aimed at driving TAMs toward M1 polarization have shown promise in mouse models of cancer (Georgoudaki et al., 2016; Pyonteck et al., 2013).

Recently, it was reported that CCR2+ monocyte-derived TAMs were involved not only in ECM turnover, but also in the deposition of a tumor-specific ECM that stimulates tumor progression (Afik et al., 2016). This included the synthesis of ECM components, including collagens. In our transcriptomic comparison of carcinoma cells, fibroblasts, and collagen-endocytosing TAMs from subcutaneous LLC, we, however, observed very little contribution from TAMs to the generation of a tumor-specific ECM. Tumor-associated fibroblasts were the dominant producers of collagen, proteoglycans, and other ECM glycoproteins, whereas tumor cells expressed high levels of some proteoglycans and a few glycoproteins. Consequently, TAMs may encompass distinct subpopulations involved in ECM degradation and synthesis, respectively.

IL-4-induced M2 polarization of macrophages within the tumor microenvironment upregulates cysteine cathepsins, which may function both in the lysosome and as secreted enzymes to promote ECM turnover (Olson and Joyce, 2015). Our study shows that collagen-endocytosing TAMs, in addition to high levels of cathepsins, express a range of ECM-degrading

(D and E) Flow cytometry dot plots of single-cell suspensions of LLC. Cells were FACS sorted into dTomato-expressing LLC cells, GFP-expressing fibroblasts (D), and F4/80+ cells endocytosing fluorescently labeled collagen (E).
(F) Principal component analysis of each biological RNA-seq replicate from total tumor RNA, isolated LLC cells, fibroblasts, or collagen-endocytosing TAMs as shown in (D) and (E).
(G and H) Heatmaps of normalized (*Z* score) RNA-seq read counts of genes encoding collagens, proteoglycans, and glycoproteins (G) and cathepsins, MMPs, and fibrinolytic factors (plasminogen activation system) (H).

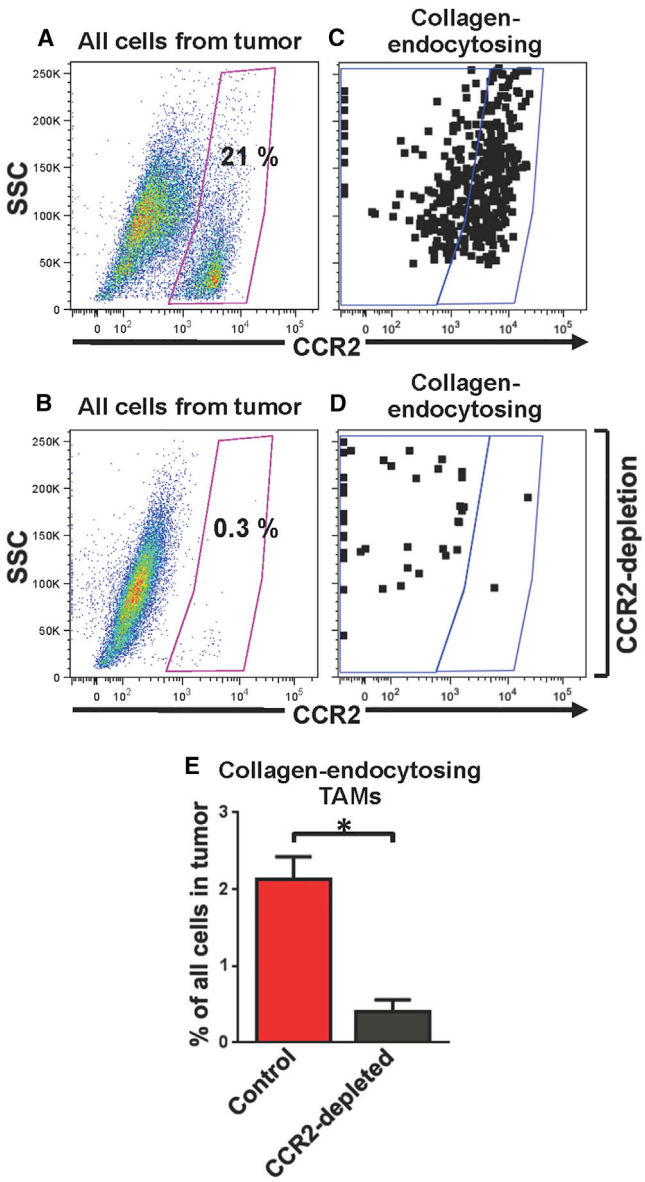

Figure 3. Collagen-Endocytosing M2-TAMs Originate from CCR2+ Monocytes

(A–D) LLC growing in *Ccr2*$^{+/RFP}$ (A and C) or *Ccr2*$^{+/RFP}$;*CCR2-depleter*$^{+/0}$ mice (B and D) treated with DT during tumor growth. *Ccr2*$^{+/RFP}$ mice are DT insensitive, whereas DT depletes CCR2+ cells in *Ccr2*$^{+/RFP}$;*CCR2-depleter*$^{+/0}$ mice. (A and C) Flow cytometry analysis of single-cell suspensions of LLC from *Ccr2*$^{+/RFP}$ mice shows that about 20% of cells in LLC are CCR2+ (A) and the majority of collagen-endocytosing TAMs (CD45+;CD11b+ cells) are CCR2+ (C). (B and D) Flow cytometry analysis of LLC from DT-treated *Ccr2*$^{+/RFP}$;*CCR2-depleter*$^{+/0}$ bi-transgenic mice demonstrates efficient depletion of CCR2+ cells (B) and removal of the vast majority of all collagen-endocytosing M2-TAMs (D). (E) Collagen-endocytosing M2-TAMs (%) in LLC from DT-treated *Ccr2*$^{+/RFP}$ mice (red bar, n = 3) or *Ccr2*$^{+/RFP}$;*CCR2-depleter*$^{+/0}$ mice (gray bar, n = 3). Error bars, SD. *p < 0.01.

enzymes, including collagenases and gelatinases. This implies that endocytic collagen turnover by TAMs may be a cell-autonomous process in which each step of the collagen catabolic sequence leading to lysosomal collagen degradation is executed by the TAMs. However, our assay, as currently configured, cannot identify the cells executing the initial collagen fragmentation. It follows that other cellular constituents of the tumor microenvironment may actively contribute to TAM-mediated endocytic collagen degradation, for example by aiding the initial collagen fragmentation. In support of this, we found high expression of the collagenase MMP-2 and its activator (and collagenase) MMP-14 in tumor-associated fibroblasts.

High expression of the elastase MMP-12 and components of the fibrinolytic system by the collagen-endocytosing TAMs suggests that other prominent constituents of the tumor ECM, such as elastin and fibrin, also may be degraded by TAMs. The degradation of such non-collagenous ECM proteins may also involve endocytosis (Motley et al., 2016).

In conclusion, we show that tumor-associated collagen degradation involves receptor-mediated endocytic uptake and lysosomal degradation of collagen by TAMs displaying a distinct matrix-catabolic signature.

EXPERIMENTAL PROCEDURES

Animal Experiments

Work was done in an American Association for Accreditation of Laboratory Animal Care (AAALAC)-certified facility with protocols approved by the National Institute of Dental and Craniofacial Research (NIDCR) Institutional Animal Care and Use Committee (NIH) or in accordance with institutional guidelines approved by the Animal Experiments Inspectorate in Denmark (Finsen Laboratory/BRIC). See the Supplemental Experimental Procedures for details on animal husbandry and genotyping.

Subcutaneous Tumors

Subcutaneous tumors were generated by injection of syngeneic C57BL/6-derived tumor cell lines as previously described (Bugge et al., 1997). See the Supplemental Experimental Procedures for details.

Histology

Tumors were fixed in zinc-buffered formalin for 24 hr, paraffin embedded, sectioned, and stained with picrosirius red. Two central areas of each tumor were selected by light microscopy, and images were acquired using polarization filters. Picrosirius red-positive areas were determined by ImageJ-based threshold-analysis. Acquisition and image analysis were blinded.

Monocyte Ablation

Mice were inoculated subcutaneously with 5 × 10^5 LLC cells and received bi-daily intraperitoneal injections of 50 ng/g body weight DT, starting on the day of inoculation and continuing until experimental endpoint 11 days later.

Collagen Labeling

Labeling of acid-extracted rat tail tendon type I collagen with fluorescent dyes was performed by modification of a previously described procedure (Birkedal-Hansen et al., 2003). See the Supplemental Experimental Procedures for details.

In Vivo Collagen Endocytosis

Mice were injected intratumorally with 80 μL of 0.4 mg/mL fluorescently labeled collagen and 0.3 mg/mL tetramethylrhodamine (TMR)-conjugated or fluorescein isothiocyanate (FITC)-conjugated 10 kDa dextran (Invitrogen) neutralized immediately before injection using HEPES-buffered PBS. 18–24 hr later, mice were injected intravenously with 150 μL of 4 mg/mL Hoechst 33342 trihydrochloride trihydrate dye (Invitrogen). Mice were euthanized 4–6 hr later, and tumors were immediately imaged by confocal microscopy.

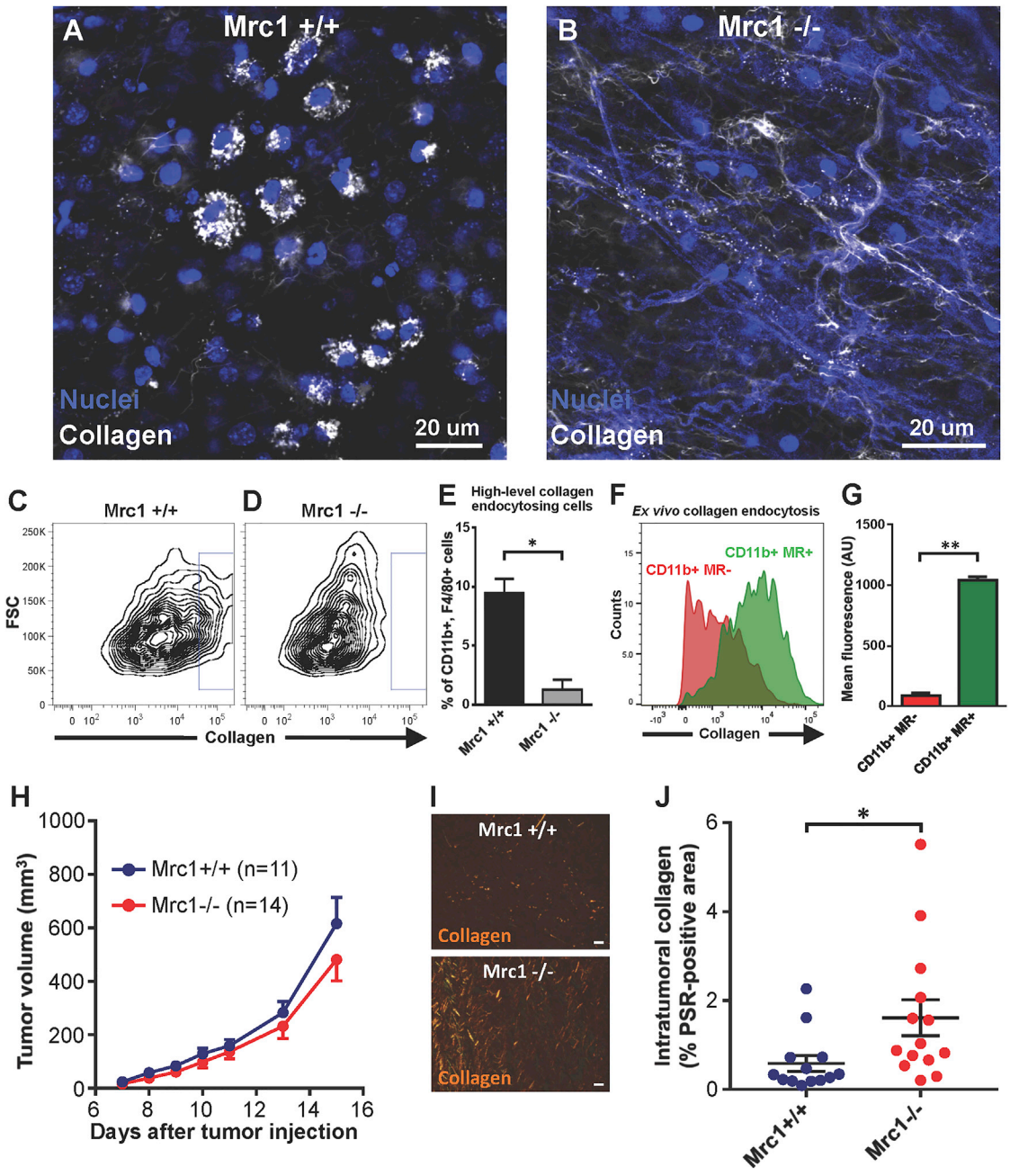

Figure 4. MR Mediates Collagen Endocytosis by M2-TAMs

(A and B) Images of collagen-injected LLC from *Mrc1*$^{+/+}$ mice (A) or *Mrc1*$^{-/-}$ littermates (B).

(C and D) Flow cytometry analysis of collagen endocytosis by CD45+; F4/80+ cells from LLC grown in *Mrc1*$^{+/+}$ mice (C) or *Mrc1*$^{-/-}$ littermates (D).

(E) Percentage of CD45+;CD11b+;F4/80+ cells from *Mrc1*$^{+/+}$ mice (black bar, n = 3) and *Mrc1*$^{-/-}$ littermates (gray bar, n = 3) with high collagen endocytosis based on flow cytometry analyses as exemplified in (C) and (D). Error bars, SD. *p < 0.01.

(F and G) Single-cell suspension of LLC tumors were enriched for CD45+ cells and sorted into CD11b+;MR− (red) and CD11b+;MR+ (green) cells. Plastic-adhered cells were incubated with Alexa 647-labeled collagen and analyzed by flow cytometry (F). Flow cytometry quantification (G). Error bars, SD. **p < 0.001.

(H) *Mrc1*$^{+/+}$ mice (blue line) and *Mrc1*$^{-/-}$ littermates (red line) were inoculated subcutaneously with LLC cells, and tumor sizes were measured from the appearance of the first palpable tumor until the largest tumor had reached the maximal permitted size. Error bars, SEM.

(I) Images from picrosirius red-stained LLC sections from *Mrc1*$^{+/+}$ mice (upper panel) or *Mrc1*$^{-/-}$ littermates (lower panel) showing collagen fibers. Bars, 50 μm.

(J) Quantification of picrosirius red (PSR)-positive areas of LLC from *Mrc1*$^{+/+}$ mice (blue dots) or from *Mrc1*$^{-/-}$ littermates (red dots). Data are individual values for each tumor, means, and SEM. *p < 0.05. **p < 0.001.

Confocal Microscopy

Confocal imaging was performed using a confocal microscope (IX81; Olympus) equipped with a scanning head (FluoView 1000; Olympus). All images were acquired using a U Plan S Apochromat 60× numerical aperture, 1.2 water-immersion objective. See the Supplemental Experimental Procedures for details.

Quantitation of Cellular Collagen and Dextran Uptake

Four z stacks of 27-μm sections were collected for each mouse, and each stack was taken from the same depth within the tissue. The total number of cells in each z stack was determined by counting all nuclei stained with Hoechst dye. Final values for cell numbers per mouse were the mean of four z stacks.

In Situ Staining

Tumors were fixed for 4 hr in zinc-buffered formalin 24 hr after collagen and dextran injection. For MR staining, tumors were permeabilized with 1% Triton X-100 in PBS for 45 min; washed in PBS, 0.5% BSA, and 0.2% Triton X-100 (PBS-BT); blocked in PBS-BT and 2% goat serum for ≥1 hr; and incubated overnight at 4°C with primary antibody in PBS-BT and 2% goat serum at these dilutions: anti-CD11b (Biolegend) 1:200 and rat anti-MR (AbD Serotec) 1:200. Tumors were washed in PBS-BT and incubated overnight at 4°C with Alexa Fluor 488-conjugated secondary antibodies diluted at 1:500 in PBS-BT. After washing in PBS-BT, the tissue was incubated for 1 hr with Hoechst diluted at 1:10,000 in PBS-BT, washed, and imaged as described in the Confocal Microscopy section.

FACS and RNA Isolation

Alexa 647-collagen and TMR-dextran were injected into LLC as described above. Tumors were harvested 24 hr later, and single-cell suspensions were prepared. Cells were blocked with Fc receptor-blocking reagent and enriched for CD45+ cells using magnetic anti-CD45 microbeads (Miltenyi). Cells were stained with Zombie aqua and anti-CD11b antibody (cl. M1/70, Biolegend) for 1 hr on ice, gated for the Zombie aqua-negative and CD11b+ cell population, and sorted into dextran- and collagen-endocytosing cells and dextran- and collagen-non-endocytosing cells on a FACS Aria II (BD Biosciences). 1 to 2×10^5 cells of each of the two cell populations were isolated from each sample. In other experiments, Alexa 647-collagen was injected into dTomato-expressing LLC growing in *Col1a1*-GFP mice. 24 hr later, single-cell suspensions were prepared, Fc receptor blocked, and stained with Zombie aqua and anti-F4/80 antibody. Cells were sorted into dTomato+ cells (cancer cells), GFP+ cells (fibroblasts), and dTomato-;GFP−;F4/80+;collagen+ cells (M2-TAMs). RNA was isolated by Trizol (Invitrogen) lysis, phase separation with chloroform, and purification using a QIAGEN RNA micro purification kit.

qPCR

100 ng total RNA was used for oligo(dT)-mediated first-strand cDNA synthesis (Superscript III First-Strand Synthesis SuperMix; Invitrogen). Gene expression analysis was performed in cell populations from 3 individual tumors using the real-time PCR detection system (iCycler iQ; Bio-Rad Laboratories) and iQ SYBR Green Supermix (Bio-Rad Laboratories). Primers are in Table S2. Details on PCR and data analysis are in the Supplemental Experimental Procedures.

RNA-Seq

RNA quality was assessed by Agilent 2100 Bioanalyzer. Total RNA (200 ng) was prepared using polydT-mediated cDNA synthesis in accordance with the manufacturer's (Illumina) instructions. Libraries were made with a NEBNext RNA Library Preparation Kit for Illumina. Library quality was assessed using Fragment Analyzer (AATI), followed by library quantification (Illumina Library Quantification Kit). Sequencing was done on a HiSeq1500 platform (Illumina) with a read length of 50 bp. Sequencing depth and alignment information is in Table S3. Details on data analysis are in the Supplemental Experimental Procedures.

Ex Vivo Collagen Endocytosis

Single-cell suspensions of LLC cells were enriched for CD45+ cells and stained with Zombie aqua, anti-CD11b (Biolegend), and anti-MR (Biolegend) antibodies as described above. Cells were sorted into CD11b+;MR+ and CD11b+;MR− cells using a FACS Aria I (BD Biosciences) and plated in 24-well plates (5 to 9×10^4 cells/well). Alexa 647-labeled collagen was added overnight at a final concentration of 15 μg/mL. Cells were trypsinized, stained with Zombie aqua, and analyzed by flow cytometry with a LSRII flow cytometer (BD Biosciences).

Statistics

Significance was tested by unpaired 2-tailed Student's t test, assuming independent variables, normal distribution, and equal variance of samples. Calculations were made with GraphPad Prism software.

DATA AND SOFTWARE AVAILABILITY

The accession number for the RNA-seq data reported in this study is GEO: GSE107053.

SUPPLEMENTAL INFORMATION

Supplemental Information includes Supplemental Experimental Procedures, two figures, and three tables and can be found with this article online at https://doi.org/10.1016/j.celrep.2017.12.011.

ACKNOWLEDGMENTS

We thank Mary Jo Danton for reviewing this manuscript. This work was supported by the NIDCR Intramural Research Program (Z01DE0699-05) (to T.H.B.), the European Commission/Marie Curie Program (659994) (to D.H.M.), Danish Cancer Society (R124-A7599-15-S2 and R90-A5989-B526) (to D.H.M. and H.J.J.), Region Hovedstadens Forskningsfond (R144-A5439) (to D.H.M.), the Novo Nordisk Foundation (NNF16OC0022922 and NNF16OC0020796) (to D.H.M. and L.G.), and the Danish Council for Independent Research (4002-00370 and 4092-00387B) (to L.G. and H.J.J). We thank Ronni Nielsen (University of Southern Denmark) for assistance with Illumina sequencing. This research was supported by the NIDCR Veterinary Research Core and Combined Technical Research Core (Z numbers DE000729-08 and DE000740-05).

AUTHOR CONTRIBUTIONS

Conceptualization, D.H.M. and T.H.B.; Methodology, D.H.M., L.G., R.W., and T.H.B.; Investigation, D.H.M., H.J.J., M.S.S., D.E.K., L.G.C., S.L., and L.G.; Writing – Original Draft, D.H.M. and T.H.B., Writing – Review & Editing, D.H.M., H.J.J., M.S.S., D.E.K., L.G.C., S.L., L.G., N.B., R.W., and T.H.B.

DECLARATION OF INTERESTS

The authors declare no competing interests.

Received: March 7, 2017
Revised: October 25, 2017
Accepted: December 3, 2017
Published: December 26, 2017

REFERENCES

Afik, R., Zigmond, E., Vugman, M., Klepfish, M., Shimshoni, E., Pasmanik-Chor, M., Shenoy, A., Bassat, E., Halpern, Z., Geiger, T., et al. (2016). Tumor macrophages are pivotal constructors of tumor collagenous matrix. J. Exp. Med. *213*, 2315–2331.

Aimes, R.T., and Quigley, J.P. (1995). Matrix metalloproteinase-2 is an interstitial collagenase. Inhibitor-free enzyme catalyzes the cleavage of collagen fibrils and soluble native type I collagen generating the specific 3/4- and 1/4-length fragments. J. Biol. Chem. *270*, 5872–5876.

Birkedal-Hansen, H. (1987). Catabolism and turnover of collagens: collagenases. Methods Enzymol. *144*, 140–171.

Birkedal-Hansen, H., Yamada, S., Windsor, J., Poulsen, A.H., Lyons, G., Stetler-Stevenson, W., and Birkedal-Hansen, B. (2003). Matrix metalloproteinases. Curr. Protoc. Cell Biol. *Chapter 10*, Unit 10.8.

Biswas, S.K., Allavena, P., and Mantovani, A. (2013). Tumor-associated macrophages: functional diversity, clinical significance, and open questions. Semin. Immunopathol. *35*, 585–600.

Bugge, T.H., Kombrinck, K.W., Xiao, Q., Holmbäck, K., Daugherty, C.C., Witte, D.P., and Degen, J.L. (1997). Growth and dissemination of Lewis lung carcinoma in plasminogen-deficient mice. Blood *90*, 4522–4531.

Danø, K., Andreasen, P.A., Grøndahl-Hansen, J., Kristensen, P., Nielsen, L.S., and Skriver, L. (1985). Plasminogen activators, tissue degradation, and cancer. Adv. Cancer Res. *44*, 139–266.

De Palma, M., Venneri, M.A., Galli, R., Sergi Sergi, L., Politi, L.S., Sampaolesi, M., and Naldini, L. (2005). Tie2 identifies a hematopoietic lineage of proangiogenic monocytes required for tumor vessel formation and a mesenchymal population of pericyte progenitors. Cancer Cell *8*, 211–226.

Engelholm, L.H., List, K., Netzel-Arnett, S., Cukierman, E., Mitola, D.J., Aaronson, H., Kjøller, L., Larsen, J.K., Yamada, K.M., Strickland, D.K., et al. (2003). uPARAP/Endo180 is essential for cellular uptake of collagen and promotes fibroblast collagen adhesion. J. Cell Biol. *160*, 1009–1015.

Everts, V., and Beertsen, W. (1992). Phagocytosis of collagen fibrils by periosteal fibroblasts in long bone explants. Effect of concanavalin A. Tissue Cell *24*, 935–941.

Everts, V., Beertsen, W., and Tigchelaar-Gutter, W. (1985). The digestion of phagocytosed collagen is inhibited by the proteinase inhibitors leupeptin and E-64. Coll. Relat. Res. *5*, 315–336.

Franklin, R.A., Liao, W., Sarkar, A., Kim, M.V., Bivona, M.R., Liu, K., Pamer, E.G., and Li, M.O. (2014). The cellular and molecular origin of tumor-associated macrophages. Science *344*, 921–925.

Freije, J.M., Díez-Itza, I., Balbín, M., Sánchez, L.M., Blasco, R., Tolivia, J., and López-Otín, C. (1994). Molecular cloning and expression of collagenase-3, a novel human matrix metalloproteinase produced by breast carcinomas. J. Biol. Chem. *269*, 16766–16773.

Georgoudaki, A.-M., Prokopec, K.E., Boura, V.F., Hellqvist, E., Sohn, S., Östling, J., Dahan, R., Harris, R.A., Rantalainen, M., Klevebring, D., et al. (2016). Reprogramming tumor-associated macrophages by antibody targeting inhibits cancer progression and metastasis. Cell Rep. *15*, 2000–2011.

Gocheva, V., Wang, H.-W., Gadea, B.B., Shree, T., Hunter, K.E., Garfall, A.L., Berman, T., and Joyce, J.A. (2010). IL-4 induces cathepsin protease activity in tumor-associated macrophages to promote cancer growth and invasion. Genes Dev. *24*, 241–255.

Hasty, K.A., Jeffrey, J.J., Hibbs, M.S., and Welgus, H.G. (1987). The collagen substrate specificity of human neutrophil collagenase. J. Biol. Chem. *262*, 10048–10052.

Hotary, K., Allen, E., Punturieri, A., Yana, I., and Weiss, S.J. (2000). Regulation of cell invasion and morphogenesis in a three-dimensional type I collagen matrix by membrane-type matrix metalloproteinases 1, 2, and 3. J. Cell Biol. *149*, 1309–1323.

Hotary, K., Li, X.Y., Allen, E., Stevens, S.L., and Weiss, S.J. (2006). A cancer cell metalloprotease triad regulates the basement membrane transmigration program. Genes Dev. *20*, 2673–2686.

Hughes, R., Qian, B.-Z., Rowan, C., Muthana, M., Keklikoglou, I., Olson, O.C., Tazzyman, S., Danson, S., Addison, C., Clemons, M., et al. (2015). Perivascular M2 macrophages stimulate tumor relapse after chemotherapy. Cancer Res. *75*, 3479–3491.

Hynes, R.O. (2009). The extracellular matrix: not just pretty fibrils. Science *326*, 1216–1219.

Jones, P.A., and De Clerck, Y.A. (1982). Extracellular matrix destruction by invasive tumor cells. Cancer Metastasis Rev. *1*, 289–317.

Kaukonen, R., Mai, A., Georgiadou, M., Saari, M., De Franceschi, N., Betz, T., Sihto, H., Ventelä, S., Elo, L., Jokitalo, E., et al. (2016). Normal stroma suppresses cancer cell proliferation via mechanosensitive regulation of JMJD1a-mediated transcription. Nat. Commun. *7*, 12237.

Kjøller, L., Engelholm, L.H., Høyer-Hansen, M., Danø, K., Bugge, T.H., and Behrendt, N. (2004). uPARAP/endo180 directs lysosomal delivery and degradation of collagen IV. Exp. Cell Res. *293*, 106–116.

Knäuper, V., López-Otin, C., Smith, B., Knight, G., and Murphy, G. (1996). Biochemical characterization of human collagenase-3. J. Biol. Chem. *271*, 1544–1550.

Lahmar, Q., Keirsse, J., Laoui, D., Movahedi, K., Van Overmeire, E., and Van Ginderachter, J.A. (2016). Tissue-resident versus monocyte-derived macrophages in the tumor microenvironment. Biochim. Biophys. Acta *1865*, 23–34.

Lee, W., Sodek, J., and McCulloch, C.A. (1996). Role of integrins in regulation of collagen phagocytosis by human fibroblasts. J. Cell. Physiol. *168*, 695–704.

Lee, H., Overall, C.M., McCulloch, C.A., and Sodek, J. (2006). A critical role for the membrane-type 1 matrix metalloproteinase in collagen phagocytosis. Mol. Biol. Cell *17*, 4812–4826.

Lewis, C.E., Harney, A.S., and Pollard, J.W. (2016). The multifaceted role of perivascular macrophages in tumors. Cancer Cell *30*, 18–25.

Linsenmayer, T.F. (1991). Collagen. In Cell Biology of Extracellular Matrix, E.D. Hay, ed. (Springer), pp. 7–44.

Liotta, L.A., Rao, C.N., and Barsky, S.H. (1983). Tumor invasion and the extracellular matrix. Lab. Invest. *49*, 636–649.

Lohela, M., Casbon, A.-J., Olow, A., Bonham, L., Branstetter, D., Weng, N., Smith, J., and Werb, Z. (2014). Intravital imaging reveals distinct responses of depleting dynamic tumor-associated macrophage and dendritic cell subpopulations. Proc. Natl. Acad. Sci. USA *111*, E5086–E5095.

Lu, P., Weaver, V.M., and Werb, Z. (2012). The extracellular matrix: a dynamic niche in cancer progression. J. Cell Biol. *196*, 395–406.

Madsen, D.H., Engelholm, L.H., Ingvarsen, S., Hillig, T., Wagenaar-Miller, R.A., Kjøller, L., Gårdsvoll, H., Høyer-Hansen, G., Holmbeck, K., Bugge, T.H., and Behrendt, N. (2007). Extracellular collagenases and the endocytic receptor, urokinase plasminogen activator receptor-associated protein/Endo180, cooperate in fibroblast-mediated collagen degradation. J. Biol. Chem. *282*, 27037–27045.

Madsen, D.H., Ingvarsen, S., Jürgensen, H.J., Melander, M.C., Kjøller, L., Moyer, A., Honoré, C., Madsen, C.A., Garred, P., Burgdorf, S., et al. (2011). The non-phagocytic route of collagen uptake: a distinct degradation pathway. J. Biol. Chem. *286*, 26996–27010.

Madsen, D.H., Jürgensen, H.J., Ingvarsen, S., Melander, M.C., Vainer, B., Egerod, K.L., Hald, A., Rønø, B., Madsen, C.A., Bugge, T.H., et al. (2012). Endocytic collagen degradation: a novel mechanism involved in protection against liver fibrosis. J. Pathol. *227*, 94–105.

Madsen, D.H., Leonard, D., Masedunskas, A., Moyer, A., Jürgensen, H.J., Peters, D.E., Amornphimoltham, P., Selvaraj, A., Yamada, S.S., Brenner, D.A., et al. (2013). M2-like macrophages are responsible for collagen degradation through a mannose receptor-mediated pathway. J. Cell Biol. *202*, 951–966.

Martinez-Pomares, L., Wienke, D., Stillion, R., McKenzie, E.J., Arnold, J.N., Harris, J., McGreal, E., Sim, R.B., Isacke, C.M., and Gordon, S. (2006). Carbohydrate-independent recognition of collagens by the macrophage mannose receptor. Eur. J. Immunol. *36*, 1074–1082.

Motley, M.P., Madsen, D.H., Jürgensen, H.J., Spencer, D.E., Szabo, R., Holmbeck, K., Flick, M.J., Lawrence, D.A., Castellino, F.J., Weigert, R., and Bugge, T.H. (2016). A CCR2 macrophage endocytic pathway mediates extravascular fibrin clearance in vivo. Blood *127*, 1085–1096.

Naba, A., Clauser, K.R., Lamar, J.M., Carr, S.A., and Hynes, R.O. (2014). Extracellular matrix signatures of human mammary carcinoma identify novel metastasis promoters. eLife *3*, e01308.

Netzel-Arnett, S., Mitola, D.J., Yamada, S.S., Chrysovergis, K., Holmbeck, K., Birkedal-Hansen, H., and Bugge, T.H. (2002). Collagen dissolution by keratinocytes requires cell surface plasminogen activation and matrix metalloproteinase activity. J. Biol. Chem. *277*, 45154–45161.

Noy, R., and Pollard, J.W. (2014). Tumor-associated macrophages: from mechanisms to therapy. Immunity *41*, 49–61.

Olson, O.C., and Joyce, J.A. (2015). Cysteine cathepsin proteases: regulators of cancer progression and therapeutic response. Nat. Rev. Cancer *15*, 712–729.

Pyonteck, S.M., Akkari, L., Schuhmacher, A.J., Bowman, R.L., Sevenich, L., Quail, D.F., Olson, O.C., Quick, M.L., Huse, J.T., Teijeiro, V., et al. (2013). CSF-1R inhibition alters macrophage polarization and blocks glioma progression. Nat. Med. *19*, 1264–1272.

Ricard-Blum, S., and Ville, G. (1989). Collagen cross-linking. Int. J. Biochem. *21*, 1185–1189.

Schedin, P., and Keely, P.J. (2011). Mammary gland ECM remodeling, stiffness, and mechanosignaling in normal development and tumor progression. Cold Spring Harb. Perspect. Biol. *3*, a003228.

Sloane, B.F., and Honn, K.V. (1984). Cysteine proteinases and metastasis. Cancer Metastasis Rev. *3*, 249–263.

Stricklin, G.P., Bauer, E.A., Jeffrey, J.J., and Eisen, A.Z. (1977). Human skin collagenase: isolation of precursor and active forms from both fibroblast and organ cultures. Biochemistry *16*, 1607–1615.

Zhang, Q.W., Liu, L., Gong, C.Y., Shi, H.S., Zeng, Y.H., Wang, X.Z., Zhao, Y.W., and Wei, Y.Q. (2012). Prognostic significance of tumor-associated macrophages in solid tumor: a meta-analysis of the literature. PLoS ONE *7*, e50946.